

Nuclear Instruments and Methods 00 (1982) NIM 0506U  
 North-Holland Publishing Company

198, ~~3~~ (1982) 33

Part II. Ion induced desorption of biomolecules

TIME-OF-FLIGHT MEASUREMENTS OF SECONDARY ORGANIC IONS PRODUCED BY 1 keV TO 16 keV PRIMARY IONS

K.G. STANDING, B.T. CHAIT\*, W. ENS, G. McINTOSH and R. BEAVIS

Physics Department, University of Manitoba Winnipeg, Canada R3T 2N2

The Manitoba time-of-flight mass spectrometer is described briefly. Relative yields for the prominent ions in the secondary ion spectrum of the amino acid alanine have been measured for primary alkali ions ( $\text{Cs}^+$ ,  $\text{K}^+$ ,  $\text{Na}^+$  and  $\text{Li}^+$ ) at energies from 1 keV to 16 keV. Yields increase greatly with increasing energy and with the mass of the bombarding particle, suggesting that in this energy region the nuclear stopping is mainly responsible for the secondary ion production.

Introduction—the mass spectrometer

The Manitoba time-of-flight mass spectrometer [1] is shown schematically in fig. 1. It is similar to the instrument of Macfarlane and Torgerson [2], but with the addition of the pulsed ion gun shown in fig. 2. Here alkali metal ions ( $\text{Li}^+$ ,  $\text{Na}^+$ ,  $\text{K}^+$  or  $\text{Cs}^+$ ) are thermionically emitted from a small glassy bead of alkali aluminosilicate [3,4] melted onto the end of a tungsten hairpin filament. This simple ion source has proven very satisfactory; it creates negligible gas load, provides ions of a variety of masses, and yields ample current for our modest needs. The source has operated thus far at potentials  $V_p$  up to 25 kV, corresponding to an ion energy of 25 keV.

The ion beam is focused by a gridded einzel lens to a spot of about  $100 \mu\text{m}$  diameter in the

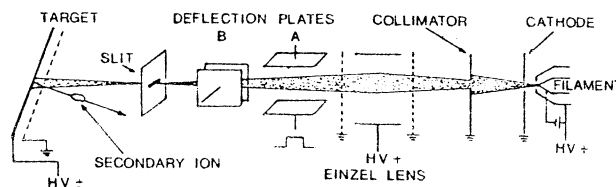


Fig. 2. Pulsed positive ion source.

plane containing the defining slit. It is swept rapidly across the  $35 \mu\text{m}$  wide slit by a voltage pulse applied to the deflection plates A. The duration of the ion burst passing through the slit has varied from  $\sim 4 \text{ ns}$  to  $\sim 50 \text{ ns}$ , depending on the energy, the ion species, and the deflecting voltage.

The primary ion beam strikes the target at an angle of incidence of approximately  $20^\circ$ . Either positive or negative secondary ions may be observed by simply reversing the potential  $V_s$  applied to the target. For positive secondary ions,  $V_s = +|V|$  and the energy of the primary ion (charge  $q_p$ ) at the target is  $q_p (V_p - |V|)$ . For negative secondary ions,  $V_s = -|V|$  and the primary ion energy at the target is  $q_p (V_p + |V|)$ .

The secondary ions are detected by chevron microchannel electron multiplier (1.8 cm or 4.0 cm in diameter) at the end of the 1.6 m flight tube. Time-of-flight is measured by conventional nuclear timing circuits as shown in fig. 3. For detailed observation of the high mass region, a fixed delay is inserted before the TAC start, as in the example shown in the figure. With this arrangement the non-linearity and jitter produced by the analogue

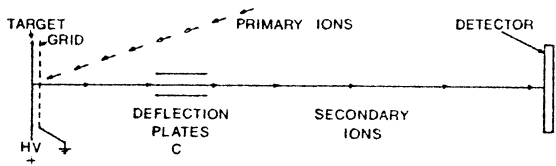


Fig. 1. Schematic diagram of the time-of-flight mass spectrometer (not to scale). The deflection plates C actually consist of two adjacent pairs of plates to give independent horizontal and vertical deflections.

IMPORTANT

1. Please correct proofs carefully
2. Restrict corrections to instances in which the proof

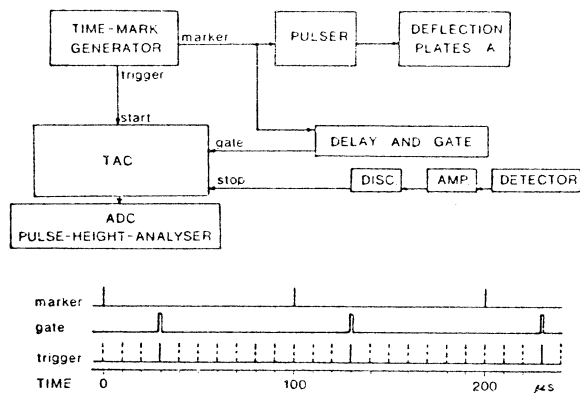


Fig. 3. Schematic diagram of the timing circuits. The example above shows the timing sequence for primary pulses separated by  $100 \mu\text{s}$  and the TAC start delayed by  $30 \mu\text{s}$ . The ungated "trigger" pulses are shown as dashed lines; pulses separated by  $10 \mu\text{s}$  are shown for clarity, although the normal separation used was  $1 \mu\text{s}$ . Since the error in "trigger" timing is determined by the stability of the 10 MHz reference oscillator in the time-mark generator (Tektronix 184), specified as 0.0003% in 24 hr, the starting error in the delayed sweep is very small.

TAC and ADC circuits are greatly reduced. The TAC dead time produced by the predominant low mass ions is also eliminated.

The TAC dead time still provides the basic limitation in the counting rate. Since the TAC can measure only one ion per sweep, the probability of two ions being produced within its time range by a single primary pulse must be kept small. This limits the usable primary beam. In spite of this limitation spectra may be obtained within reasonable times - 10 to 80 min for a sample of high molecular weight.

Under various operating conditions, the dc current extracted from the ion source ranges from 0.3 nA to 30 nA. Normally the beam is adjusted so that  $\sim 100$  to  $\sim 1000$  ions per pulse pass through the slit and hit the target, at a repetition frequency of 5 to 10 kHz. This corresponds to an average ion current  $\sim 0.1 \text{ pA}$  to  $\sim 1 \text{ pA}$  on the target. The target beam spot has a diameter  $\sim 2 \text{ mm}$ , so the average ion current density on the beam spot is  $\sim 3$  to  $\sim 30 \text{ pA/cm}^2$ , several orders of magnitude smaller than current densities typically used with magnetic and quadrupole instruments. We note particularly that our beam current is a factor  $\sim 10^7$  lower than the current used in recently reported measurements with "fast atom bombardment" [5], where secondary ions were produced by

a neutral primary beam and examined in a magnetic spectrometer. Since the ultimate sensitivity of any technique involving particle bombardment is probably limited by radiation damage in the target, these numbers have obvious implications.

To date this instrument has been used in a direct comparison of the secondary ion mass spectra produced by fission fragments and low energy ions [6,7]. It has also been used to study in some detail the mass spectra from a series of eight fully protected ribodinucleotides of masses  $\sim 1100$  to  $\sim 1400 \text{ u}$  [8] and from two neuropeptides [9]. Significant yields of quasi-molecular ions have been obtained from intractable compounds such as vitamin B12, and from protected nucleotides of masses up to  $\sim 2100 \text{ u}$ . Here we report some measurements on a simple amino acid (alanine), which may shed some light on the mechanism of the desorption process.

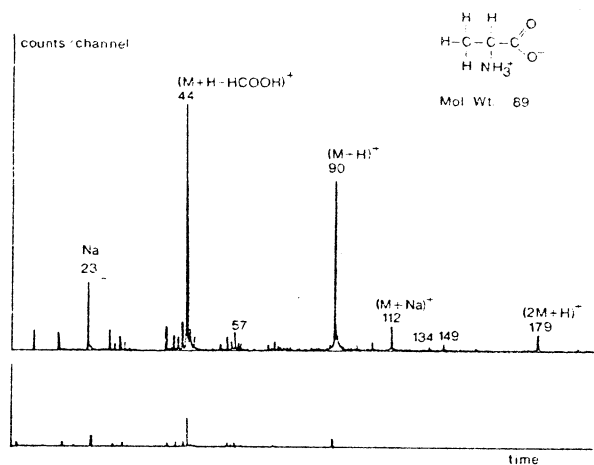
## 2. Experimental measurements

Samples of alanine\* were dissolved in methanol + 10% water (no other additions), then electro-sprayed [10] onto aluminized polyester film to give a sample thickness  $\sim 40 \mu\text{g/cm}^2$ . A typical time-of-flight spectrum is shown in the upper part of fig. 4. The most prominent lines correspond to the alanine quasi-molecular ion at mass 90, the alanine fragment at mass 44, and the  $\text{Na}^+$  background ion at mass 23.

In order to determine the radial velocity distribution of the secondary ions leaving the target, we have measured the counting rate as a function of the voltage on the deflection plates C of fig. 1. The experimental points in fig. 5 show typical results. The profiles were the same for both horizontal and vertical deflections; they were also independent of the primary ion energy. The experimental results were compared with profiles calculated for an initial radial velocity distribution of the form  $dN/dE_r = A_r e^{-\lambda_r E_r}$ , where  $E_r = \frac{1}{2} m v_r^2$ , and  $m$  and  $v_r$  are the mass and radial velocity of the ion [11]. The fringing fields of the deflection plates were taken into account [12] in the calculations.

Fig. 5 shows the profiles calculated for three values of  $\lambda_r$ ; the experimental results are con-

\* Sigma Chemical Co., St. Louis, Mo., U.S.A.



sistent with a radial distribution having a width  $1/\lambda_r = (0.22 \pm 0.03)$  eV for the alanine fragment at mass 44. The experimental points for the quasi-molecular ion were consistent with a distribution of the same width, but the  $\text{Na}^+$  ion had a narrower distribution, with  $1/\lambda_r = (0.14 \pm 0.02)$  eV. These values of  $\lambda_r$  gave profiles which fitted the experimental points for secondary ion energies between 1 and 8 keV. When the deflection plates are adjusted to centre the secondary ion beam, we calculate that  $\geq 90\%$  of the secondary ions hit our 4 cm diameter detector. The widths determined here are considerably smaller than those reported earlier by the Darmstadt group for ions released by fission fragment bombardment [11], but we understand that more recent results at Darmstadt are closer to our own [13].

We have observed pronounced variations in the

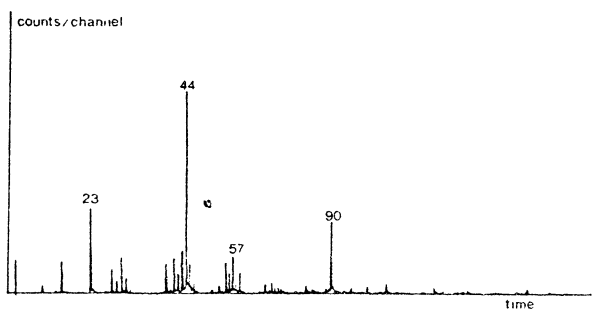


Fig. 4. Positive ion spectra for alanine at two different primary ion energies. The upper and middle spectra are shown on the same scale. The lower spectrum is the same as the middle spectrum, magnified 8 times. Upper: primary ions 14 keV  $\text{Cs}^+$ , secondary ions 4 keV, duration 1.3 min. Middle and lower: primary ions 1 keV  $\text{Cs}^+$ , secondary ions 4 keV, duration 1.7 min.

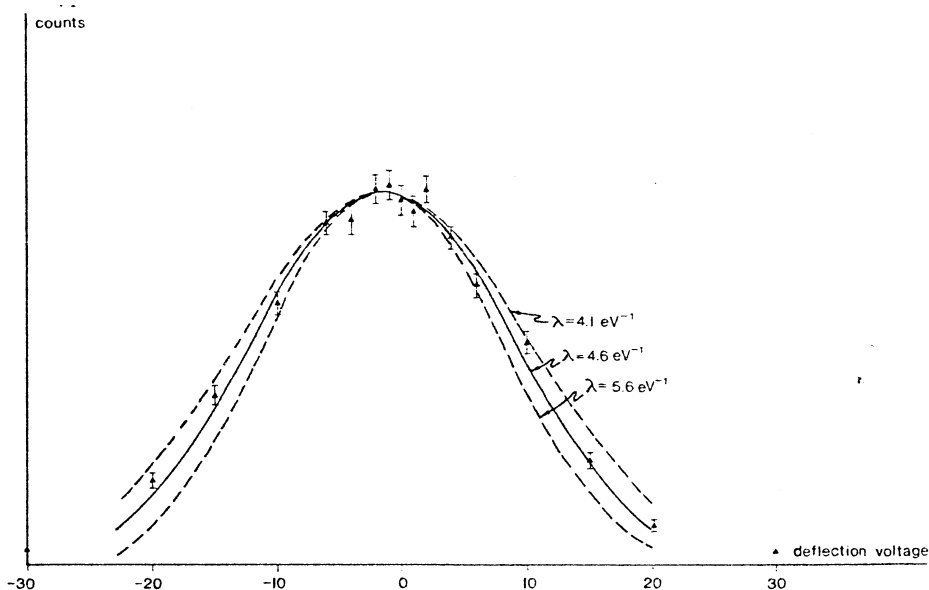


Fig. 5.  $(\text{M}+\text{H}-\text{HCOOH})^+$  secondary ions detected as a function of voltage on the deflection plates shown in fig. 1. The curves shown are those calculated for  $\lambda = 4.1, 4.6$  and  $5.8 \text{ eV}^{-1}$ . Primary ions 5 keV  $\text{Cs}^+$ , secondary ions 1 keV. The raw data is displayed with no background subtraction. The points at  $\pm 30 \text{ V}$  correspond to the background level; i.e., no distinct peaks were observed at these deflection voltages.

yield and spectra of secondary ions with changes in primary ion species and energy. The point is illustrated in the middle part of fig. 4, which shows the positive secondary ion spectrum excited by 1 keV  $\text{Cs}^+$  primary ions, as compared to the spectrum above, excited by 14 keV  $\text{Cs}^+$  ions. When the primary ion energy increases from 1 keV to 14 keV, the yield of the quasi-molecular ions increases by more than an order of magnitude, their ratio to the fragment ions increases, and cluster ions  $(2M + H)^+$  become apparent.

The most obvious parameter which varies with primary ion energy and species is the stopping power  $dE/dx$ , the energy loss per travelled path length. The stopping power has two components, "nuclear stopping" (elastic collisions with the target atoms), and "electronic stopping" (energy transfer to the atomic electrons). Both nuclear and electronic energy losses were calculated for alkali-metal ions incident on alanine using the Lindhard theory [14] as modified by Wilson, Haggmark and Biersack [15]. The results are shown in fig. 6. Clearly the nuclear and electronic energy losses behave

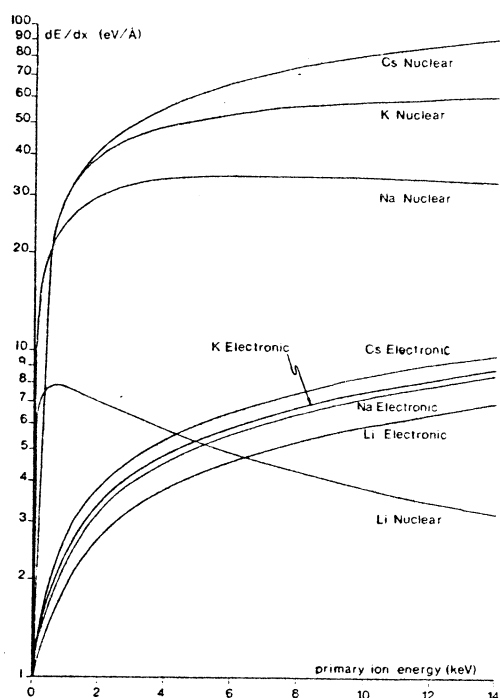


Fig. 6. Nuclear and electronic energy losses at the surface of an alanine target as a function of primary ion energy for  $\text{Li}^+$ ,  $\text{Na}^+$ ,  $\text{K}^+$  and  $\text{Cs}^+$ . Curves were calculated using the "average" parameters quoted in ref. 15.

quite differently as the projectile is changed. The dependence on energy is also apparent.

We have measured the secondary ions from alanine produced by primary  $\text{Cs}^+$ ,  $\text{K}^+$ ,  $\text{Na}^+$  and  $\text{Li}^+$  ions at energies up to 16 keV. In these measurements the secondary ion energy was 8 keV. The number of secondary ions detected in each peak was determined by adding the counts in the corresponding channels of the pulse height analyzer. The number of primary ions hitting the target was determined by measuring the dc beam hitting the slit in fig. 2, and calculating the fraction of the beam which passes through the slit from knowledge of the geometry of the apparatus and the voltage pulse applied to the deflecting plates A. The slit forms the end of a perforated cylinder which is isolated from the rest of the ion gun. This was used as the Faraday cup for measuring the dc

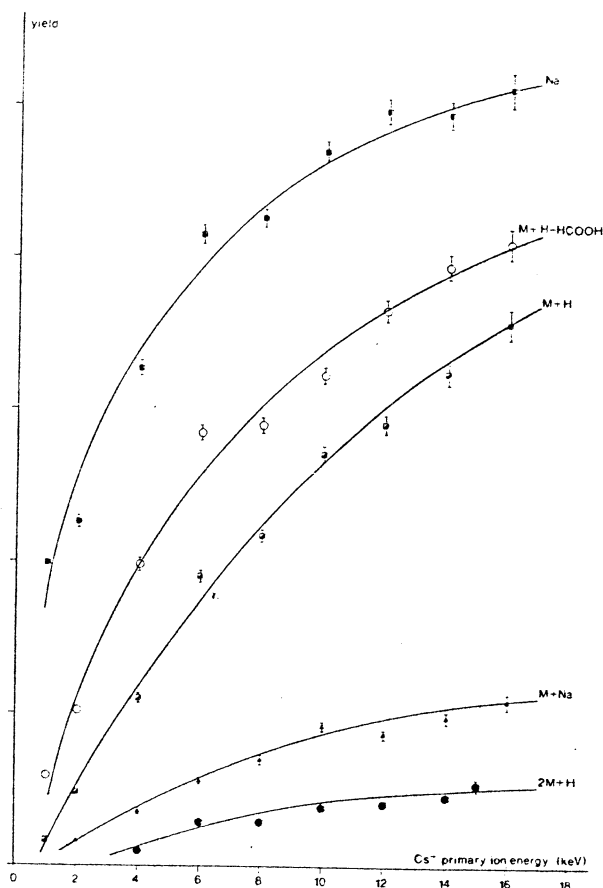


Fig. 7. Secondary ion yields from alanine produced by  $\text{Cs}^+$  primary ions.

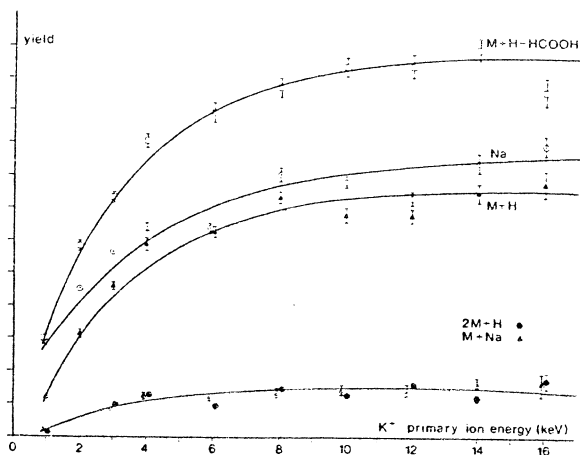


Fig. 8. Secondary ion yields from alanine produced by  $K^+$  primary ions.

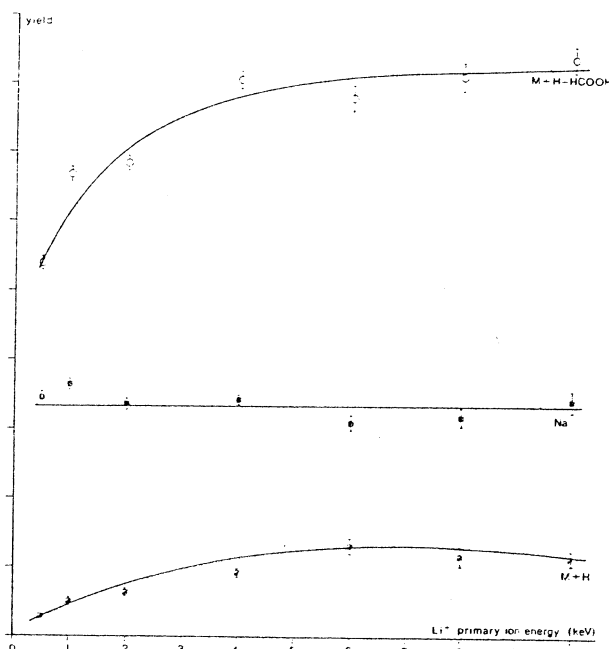


Fig. 10. Secondary ion yields from alanine produced by  $Li^+$  primary ions.

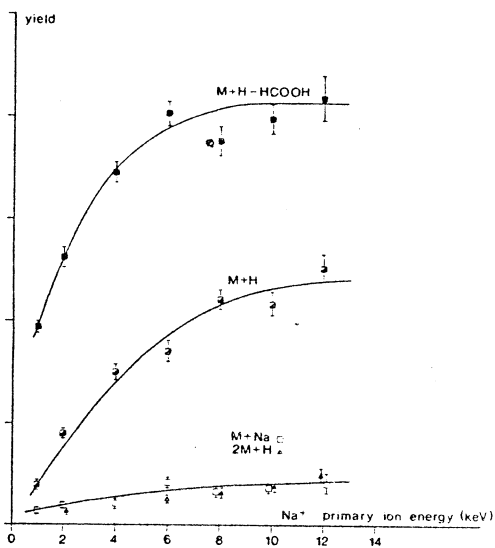


Fig. 9. Secondary ion yields from alanine produced by  $Na^+$  primary ions.

slit current\*; however, some secondary electrons may escape through the perforations, thus increasing the apparent primary current, so our estimates of absolute yields should be treated as lower limits.

Figs. 7-10 show the relative yields for various secondary ions when alanine is bombarded by

\* The current in the Faraday cup was integrated by counting the output pulses from a current-to-frequency converter (Model 170, Analogue Technology Corp., Irwindale CA., U.S.A.).

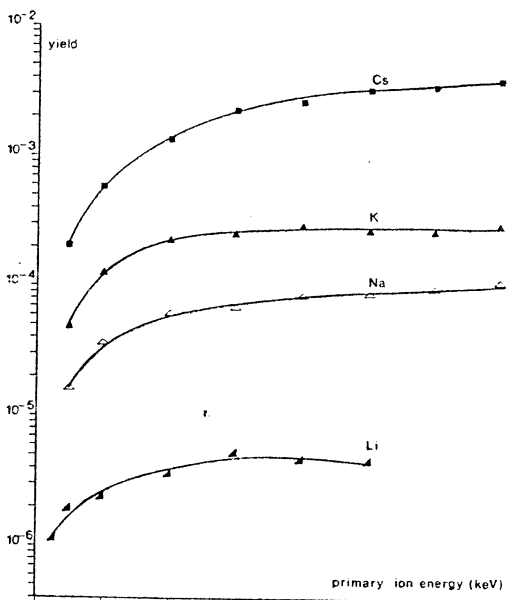


Fig. 11. Yields of  $(M+H)^+$  secondary ions from alanine produced by  $Cs^+$ ,  $K^+$ ,  $Na^+$  and  $Li^+$  primary ions. The scale gives the absolute yield (secondary ions/primary ion) estimated by the method described in the text, so the experimental points should be taken as lower limits. (Primary ion energy scale??)

$\text{Cs}^+$ ,  $\text{K}^+$ ,  $\text{Na}^+$  and  $\text{Li}^+$  ions of energies up to 16 keV. In all cases the yields increase with increasing primary energy. For the lighter ions the curves tend to flatten out between 5 keV and 10 keV, but for  $\text{Cs}^+$  the yields are still increasing at 16 keV. The ratio of the quasimolecular ion  $(\text{M} + \text{H})^+$  to the fragment ion  $(\text{M} + \text{H} - \text{HCOOH})^+$  increases with increasing primary energy and with the mass of the bombarding particle, having values  $\sim 0.1$  for 10 keV  $\text{Li}^+$ ,  $\sim 0.5$  for 2 keV  $\text{Cs}^+$  and  $\sim 0.9$  for 16 keV  $\text{Cs}^+$ . On the other hand, the ratio of the cluster ion  $(2\text{M} + \text{H})^+$  to the quasimolecular ions  $(\text{M} + \text{H})^+$  and  $(\text{M} + \text{Na})^+$  remains fairly constant (for  $\text{Na}^+$ ,  $\text{K}^+$ , and  $\text{Cs}^+$ ).

Fig. 11 shows the relative yields for the ion  $(\text{M} + \text{H})^+$  as a function of primary ion energy and species. Clearly there is a strong dependence on the mass of the incident ion.

### 3. Discussion

Comparison of the experimental yields (fig. 11) with the stopping powers (fig. 6) suggests that it is the nuclear energy loss (or perhaps the total energy loss) which is responsible for the production of secondary ions in our energy region. This is in contrast to the high energy (MeV) region, where the electronic stopping must be responsible for the observed production. Thus it appears that *both* mechanisms of energy loss are effective in producing secondary organic ions, as suggested also by results reported at this symposium by Dück and Håkansson.

Our experimental yields are consistent qualitatively with those expected from sputtering theory, assuming a combination of sputtering from linear cascades and from non-linear thermal spikes [16–18]. We note that during the whole series of measurements a total of  $\approx 10^{12}$  ions/cm<sup>2</sup> were incident on the target.

The constant ratio observed between the yield of clusters  $(2\text{M} + \text{H})$  and the yield of quasimolecular ions  $(\text{M} + \text{H})$  contradicts the result predicted if the cluster were formed in front of the surface by two molecules emitted independently; in that case the yield would be expected to vary as the square of the number of molecules emitted in an individual event [16]. Thus the experimental result supports the idea that the clusters already exist on the surface and are ejected as a unit by the primary ion.

As a practical matter, it is obvious from fig. 7–11 that there are considerable advantages in bombarding the target with particles having a larger stopping power.  $\text{Cs}^+$  ions at 16 keV gave higher yields and less fragmentation than any others measured; it will be interesting to see if this behavior extends to heavier primary ions and perhaps to bombardment by cluster ions.

We thank the Natural Sciences and Engineering Research Council of Canada for financial support and for the award of graduate scholarships to R.B. and W.E., as well as an undergraduate summer research award given to G.M. We also thank Cindy Krysac for her assistance.

### References

- [1] B.T. Chait and K.G. Standing, *Int. J. Mass Spectrom. Ion Phys.* 40 (1981) 185.
- [2] R.D. Macfarlane and D.F. Torgerson, *Int. J. Mass Spectrom. Ion Phys.* 21 (1976) 81.
- [3] J.P. Blewett and E.J. Jones, *Phys. Rev.* 50 (1936) 464.
- [4] S.K. Allison and M. Tamegai, *Rev. Sci. Instr.* 32 (1961) 1090.
- [5] M. Barber, R.S. Bordoli, R.D. Sedgwick and A.N. Tyler, *J. Chem. Soc., Chem. Commun.* (1981) 325; also reports presented at the 29th Annual Conf., American Soc. for Mass Spectrometry, Minneapolis, MN., U.S.A., (May 1981).
- [6] K.G. Standing, W. Ens, B.T. Chait and F.H. Field, in *Proc. of the Internat. Conf. on Ion formation from organic solids*, Münster, F.R.G. (6–8 October 1980) ed., A. Benninghoven (Springer-Verlag, Heidelberg) in press.
- [7] W. Ens, K.G. Standing, B.T. Chait and F.H. Field, *Anal. Chem.*, 53 (1981) 1241.
- [8] W. Ens, K.G. Standing, J.B. Westmore, K.K. Ogilvie, and M.J. Nemer, submitted to *Anal. Chem.*
- [9] J.B. Westmore, W. Ens and K.G. Standing, submitted to *Biomed. Mass Spectrom.*
- [10] C.J. McNeal, R.D. Macfarlane and E.L. Thurston, *Anal. Chem.* 51 (1979) 2036.
- [11] N. Fürstenau, W. Knippelberg, F.R. Krueger, G. Weiss and K. Wien, *Z. Naturforsch.* 32 a (1977) 711.
- [12] A. Recknagel, *Z. Phys.* 111 (1938) 61.
- [13] O. Becker, private communication.
- [14] J. Lindhard, M. Scharff and H.E. Schiøtt, *Mat. Fys. Medd., Dan Vid. Selsk.* 33 (1963) no. 14.
- [15] W.D. Wilson, L.G. Haggmark and J.P. Biersack, *Phys. Rev. B* 15 (1977) 2458.
- [16] P. Sigmund in *Inelastic Ion-Surface Collisions*, eds., N.H. Tolk et al. (Academic, New York, 1977) p. 121.
- [17] P. Sigmund and C. Claussen, *Sputtering from Elastic Collision Spikes*, paper presented at the Symposium on Sputtering, Vienna (April 1980).
- [18] P. Sigmund, *J. Vac. Sci. Technol.* 17 (1980) 396.